Synaptic effects of mutations in neuronal Cav2.1 calcium channels

Kaja, S.

4

Severe and Progressive Neurotransmitter Release Aberrations in a Novel Familial Hemiplegic Migraine *Cacna1a* S218L Knock-In Mouse

Simon Kaja,[1,2] Rob C.G. van de Ven,[3] Rune R. Frants,[3] Michel D. Ferrari,[1] Arn M.J.M. van den Maagdenberg,[1,3] and Jaap J. Plomp [1,2]

Departments of [1]Neurology, [2]Molecular Cell Biology – Group Neurophysiology and [3]Human Genetics, Leiden University Medical Centre, Leiden, The Netherlands.

To be submitted

Abstract

Familial hemiplegic migraine type 1 (FHM1) is a severe subtype of migraine with aura, characterized by hemiplegia during the migraine attack and caused by mutations in the CACNA1A gene, encoding neuronal presynaptic $Ca_V2.1$ (P/Q-type) Ca^{2+} channels.

$Ca_V2.1$ channels mediate neurotransmitter release at many central synapses and at the peripheral neuromuscular junction (NMJ). The human CACNA1A S218L mutation is associated with FHM and ataxia with susceptibility to brain edema and fatal coma after minor head trauma. In order to assess functional synaptic effects of the S218L mutation, we here characterize with electrophysiological methods the acetylcholine (ACh) release at NMJs of a novel FHM1 *Cacna1a* S218L knock-in mutant mouse, displaying a phenotype of ataxia and reduced survival rate. We found pronounced neurotransmitter release aberrations, including ~12-fold increased spontaneous ACh release and a 3-fold increase in 0.3 Hz nerve stimulation evoked release under the condition of low extracellular Ca^{2+}. Halfwidth of endplate potentials was increased at many NMJs. High-rate (40 Hz) evoked ACh release was slightly reduced, however, not associated with block of neurotransmission causing weakness, as assessed with grip strength measurements and *in vitro* muscle contraction experiments. Studying animals at increasing age, we found a clear progression of synaptic deficits, including development of an increased quantal content at low-rate nerve stimulation at physiological extracellular Ca^{2+} concentration and further increases in endplate potential halfwidths. Our results strengthen the hypothesis that FHM1 mutations lead to increased Ca^{2+} influx through $Ca_V2.1$ channels and suggest a shift of activation potential in negative direction of S218L mutated $Ca_V2.1$ channels, combined with slowed inactivation kinetics. A similarly pronounced increase in neurotransmitter release at central synapses of S218L mutant mice and humans may underlie or contribute to the neurological phenotype.

Acknowledgements

The authors thank Mr. LAM Broos for technical assistance. This work was supported by grants from the Prinses Beatrix Fonds (#MAR01-0105, to JJP), the Hersenstichting Nederland (#9F01(2).24, to JJP), KNAW van Leersumfonds (to JJP), the Netherlands Organisation for Scientific Research, NWO (an EMBL travel bursary to SK, and a VICI grant 918.56.602, to MDF), a 6th Framework specific targeted research project EUROHEAD (LSHM-CT-2004-504837, to MDF) and the Center for Medical Systems Biology (CMSB) established by the Netherlands Genomics Initiative/Netherlands Organisation for Scientific Research (NGI/NWO).

Introduction

Voltage-gated Ca^{2+} (Ca_V) channels are crucial players in nervous system function. They have roles in many processes, such as neurotransmitter secretion, neuronal firing and gene expression (for reviews, see Catterall, 2000; Snutch et al., 2005).

Mutations in CACNA1A, the gene encoding $Ca_V2.1$ (P/Q-type) Ca^{2+} channels have been shown to cause human neurological diseases, such as familial hemiplegic migraine type 1 (FHM1), episodic ataxia type 2 (EA2), spinocerebellar ataxia type 6 (SCA6) and some forms of epilepsy (Ophoff et al., 1996; Zhuchenko et al., 1997; Jouvenceau et al., 2001; Imbrici et al., 2004). In Lambert-Eaton myasthenic syndrome (LEMS), a neuro-immunological disorder, auto-antibodies target $Ca_V2.1$ channels of the neuromuscular junction (NMJ) (Kim and Neher, 1988), causing muscle weakness and paralysis in patients.

One very important function of $Ca_V2.1$ channels is neurotransmitter release. In central synapses, $Ca_V2.1$ channels mediate the Ca^{2+} influx required for transmitter release either exclusively (e.g. at cerebellar Purkinje cells) or jointly with other subtypes of Ca_V2 channels (e.g. at cerebellar granule cells) (Mintz et al., 1992ab; Mintz et al., 1995). At the peripheral NMJ, acetylcholine (ACh) release is exclusively dependent on $Ca_V2.1$ channels (Uchitel et al., 1992). NMJ abnormalities have been identified in some EA2 patients with a CACNA1A mutation (Jen et al., 2001; Maselli et al., 2003a). However, no defects were found in SCA6 (Jen et al., 2001; Schelhaas et al., 2004) and in FHM1 patients with the I1811L mutation (Terwindt et al., 2004).

We have recently described a first migraine knock-in (KI) mouse model carrying the FHM1 R192Q mutation in the orthologous mouse *Cacna1a* gene (Van Den Maagdenberg et al., 2004; Kaja et al., 2005). R192Q KI mice exhibited a reduced threshold for cortical spreading depression (CSD), the mechanism underlying migraine aura, and voltage-clamp studies revealed increased Ca^{2+} influx through R192Q-mutated channels resulting from a shift in their activation voltage (Van Den Maagdenberg et al., 2004).

We have previously shown that the mouse NMJ is a suitable model system to study the effects of CACNA1A mutations on ACh release *ex vivo*. Study of ACh release at the R192Q KI NMJ revealed both an increased frequency of uniquantal (spontaneous) ACh release and significantly elevated evoked release under conditions of low Ca^{2+} (Van Den Maagdenberg et al., 2004; Kaja et al., 2005), again suggesting increased Ca^{2+} influx via the mutated presynaptic $Ca_V2.1$ channels.

The FHM1 CACNA1A S218L mutation results in a susceptibility to brain edema and fatal coma following mild head trauma, and is associated with altered cerebellar morphology and progressive cerebellar ataxia (Kors et al., 2001). Here, we generated transgenic *Cacna1a* S218L KI mice. With electrophysiological, morphological and functional analyses we here assessed function and structure of S218L KI NMJs. We observed a severe, progressive synaptic phenotype characterized by increased neurotransmitter release, likely as a result of increased presynaptic Ca^{2+} influx due to prolonged channel opening. Similar changes at central synapses may contribute to the neurological phenotype of KI mice and FHM1 patients with the S218L mutation.

Materials and Methods

Mice

Generation of the S218L mouse strain was essentially as described previously for the *Cacna1a* R192Q KI strain (Van Den Maagdenberg et al., 2004). In short, codon 218 in exon

5 of the mouse *Cacna1a* gene was modified by mutagenesis now encoding a leucine instead of a serine residue. By gene targeting approach, agouti offspring was obtained carrying the transgene. For experiments, transgenic mice were used in which the neomycin-resistance cassette was deleted using mice of the EIIA-Cre deleter strain (Lakso et al., 1996) that express Cre recombinase driven by the EIIA early promoter. Heterozygous mice (~87.5% C57BL/6Jico and ~12.5% 129Ola background) were subsequently interbred to provide litters containing the wild-type, hetero- and homozygous genotypes that were used for the experiments. Animals were maintained in the Leiden University Medical Centre vivarium on a 12-hour light/dark cycle and tested during the light phase.

Litters were genotyped after weaning. The presence of the S218L mutation was confirmed by PCR of exon 5 using primers 271 5'-CTCCATGGGAGGCACTTG-3'and 272 5'-ACCTGTCCCCTCTTCAAAGC-3' and subsequent digestion with restriction enzyme *Vsp*I as well as sequence analysis of exon 5. Mice (both female and male animals) were tested at 2, 4.5 and 12 months of age (as specified in the Results section), and wherever possible, littermates were used for testing. All experiments were carried out with the investigator blinded for genotype, and genotyping was repeated after the experiment for confirmation.

S218L KI mice had similar body weights as wild-type (data not shown), weighed before experiments.

All experiments were carried out according to Dutch law and Leiden University guidelines, and were approved by the Leiden University Animal Experiments Commission.

Ex vivo *neuromuscular junction electrophysiology*

Mice were euthanized by carbon dioxide inhalation. Phrenic nerve-hemidiaphragms, soleus and flexor digitorum brevis (FDB) muscles were dissected and mounted in standard Ringer's medium containing (in mM): NaCl 116, KCl 4.5, $CaCl_2$ 2, $MgSO_4$ 1, NaH_2PO_4 1, $NaHCO_3$ 23, glucose 11, pH 7.4) at room temperature. Intracellular recordings of miniature endplate potentials (MEPPs, the spontaneous depolarizing events due to uniquantal ACh release) and endplate potentials (EPPs, the depolarization resulting from nerve action potential-evoked ACh release) were made at NMJs at 28 °C using standard micro-electrode equipment, as described previously (Plomp et al., 1992). At least 30 MEPPs and EPPs were recorded at each NMJ, and typically 5-15 NMJs were sampled per experimental condition per mouse. Muscle action potentials were blocked by 3 μM of the selective muscle Na^+ channel blocker μ-conotoxin GIIIB (Scientific Marketing Associates, Barnet, Herts, UK). In order to record EPPs, the phrenic nerve was stimulated supra-maximally at 0.3 Hz and 40 Hz. The amplitudes of EPPs and MEPPs were normalised to –75 mV, assuming 0 mV as the reversal potential for ACh-induced current (Magleby and Stevens, 1972). The normalized EPP amplitudes were corrected for non-linear summation according to (McLachlan and Martin, 1981) with an *f* value of 0.8. Quantal content, i.e. the number of ACh quanta released per nerve impulse, was calculated by dividing the normalized and corrected mean EPP amplitude by the normalized mean MEPP amplitude.

In order to assess the possible compensatory contribution of non-$Ca_V2.1$ channels to ACh release, EPPs and MEPPs were also measured in the presence of the following specific blockers: 200 nM ω-agatoxin-IVA (P/Q-type; $Ca_V2.1$), 2.5 μM ω-conotoxin-GVIA (N-type; $Ca_V2.2$) and 1 μM SNX-482 (R-type; $Ca_V2.3$). All toxins were from Scientific Marketing Associates. Measurements were made following a 20-25 min pre-incubation with the toxin.

Because some alterations in the mutated $Ca_V2.1$ channel may only be brought to light under more critical conditions, measurements were made in 0.2 mM Ca^{2+} and upon slight hyper- or depolarization by either low (2 mM) or high (10 mM) K^+ Ringer, as well as in the

presence of 200 ng/ml of the K^+ channel blocker 3,4-diaminopyridine (DAP) (Sigma, Zwijndrecht, The Netherlands).

Grip strength assessment

Muscle strength was measured using a grip strength meter for mice (600 g range; Technical and Scientific Equipment GmbH, Bad Homburg, Germany), connected to a laptop computer. The test was carried out essentially as originally described for rats (Tilson and Cabe, 1978). The peak force of each trial was considered the grip strength. Each mouse performed five trials, each about 30 s apart. The mean value of the five trials was used for statistical analysis.

Contraction experiments

Contraction experiments were performed essentially as described previously (Plomp et al., 2000; Kaja et al., 2005). In left phrenic nerve-hemidiaphragms of mice, contractions were recorded with a force transducer (type K30, Hugo Sachs Elektronik – Harvard Apparatus GmbH, March-Hugstetten, Germany), connected via a transducer amplifier module TAM-A 705/1 (Hugo Sachs Elektronik) and a 1200 series Digitizer (Axon Instruments, Molecular Devices Group, Union City, CA) to a personal computer running Axoscope 9 (Axon Instruments). The phrenic nerve was stimulated supramaximally once every 5 min with a single stimulus and a train of 120 stimuli at 40 Hz. The muscles were incubated in Ringer's solution to which d-tubocurarine (Sigma-Aldrich, Zwijndrecht, The Netherlands) was added in increasing concentrations (1 h incubation at each concentration). The amplitude of the recorded contractions was cursor-measured in Axoscope.

α-Bungarotoxin staining and image analysis

NMJ size was determined by staining the area of ACh receptors with fluorescently labeled α-bungarotoxin (αBTx), which irreversibly binds to ACh receptors. Diaphragm preparations were pinned out and fixed in 1% paraformaldehyde (Sigma, Zwijndrecht, The Netherlands) in 0.1 M phosphate-buffered saline pH 7.4 (PBS) for 30 minutes at room temperature. Following a 30 minute wash in PBS, diaphragms were incubated in 1 μg/ml Alexa Fluor 488 conjugated αBTx (Molecular Probes, Leiden, The Netherlands) in PBS for 3 hours at room temperature. After a final washing step in PBS (30 min), NMJ-containing regions were excised and mounted on microscope slides with Citifluor AF-1 antifadent (Citifluor, London, UK). Sections were viewed under an Axioplan microscope (Zeiss, Jena, Germany). NMJs were identified on the basis of αBTx staining, under standardized camera conditions. Images of αBTx stain were stored on hard disk; quantification was carried out using ImageJ (National Institutes of Health, Bethesda, MD). In every diaphragm, 7-15 NMJs were selected randomly. Length, width and perimeter of the αBTx-stained area were measured.

Statistical analyses

In the *ex vivo* electrophysiological and fluorescence microscopical analyses we measured 5-15 NMJs per muscle per experimental condition. The muscle mean value was calculated from the means of all data points obtained at a single NMJ, and subsequently used to determine the grand muscle mean with n as the number of mice tested.

For grip-strength measurements and *ex vivo* muscle contraction experiments n is the number of mice measured.

Data is presented as grand muscle means ± s.e.m. unless stated otherwise. Possible statistical significances were assessed using paired or unpaired Student's t-tests, ANOVA (with Tukey's HSD post-hoc test). P-values ≤ 0.05 were considered statistically significant in all cases.

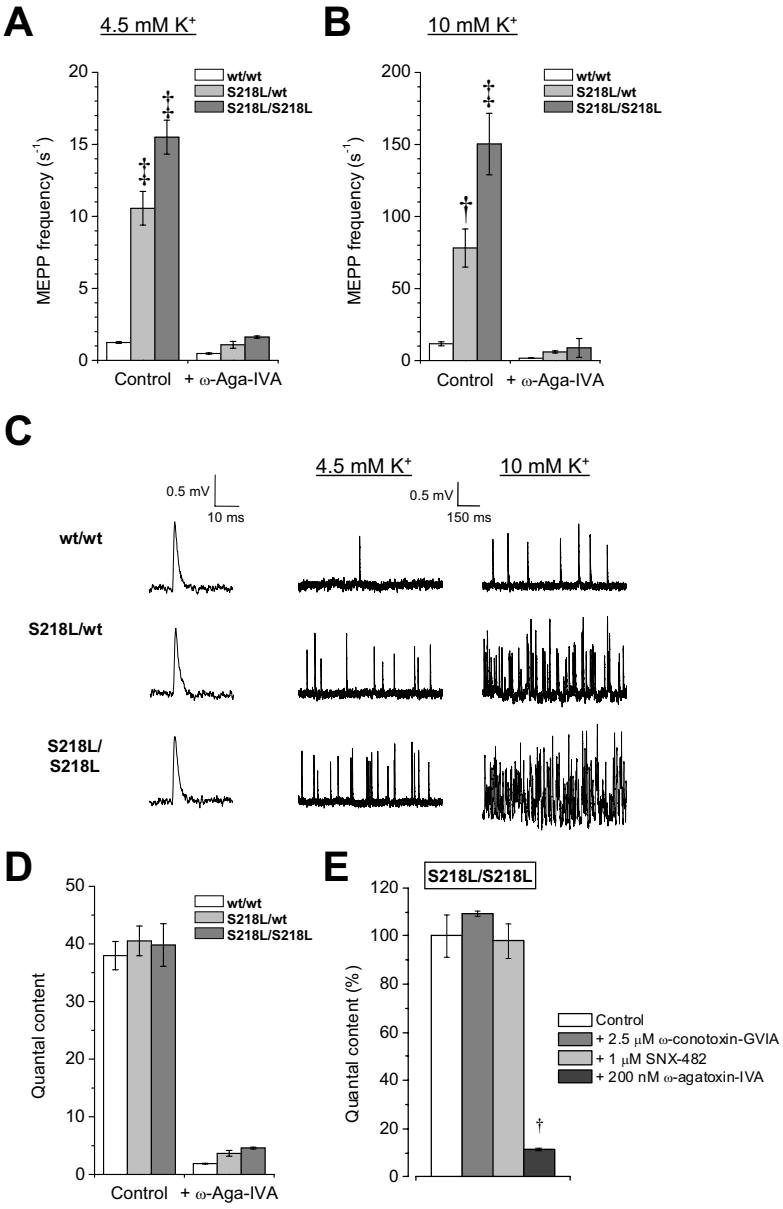

Figure 1. Gene dosage-dependent increase of spontaneous uniquantal ACh release and unchanged nerve stimulation-evoked ACh release at diaphragm NMJs of 2 months-old S218L KI mice.
(**A**) MEPP frequency is increased ~8-fold at heterozygous (S218L/wt, n=6) and ~12-fold at homozygous (S218L/S218L, n=6) S218L KI NMJs, compared to wild-type (wt/wt). The selective $Ca_V2.1$ channel blocker ω-agatoxin-IVA (200 nM) reduced MEPP frequency by ~60% at wild-type (n=3) and by >90% at both heterozygous (n=3) and homozygous (n=3) S218L KI NMJs. (**B**) Under mildly depolarizing conditions (10 mM K^+ Ringer's medium), MEPP frequency increased ~10-fold in all genotypes (n=6). ω-Agatoxin-IVA reduced MEPP frequency in all genotypes and eliminated the observed differences between genotypes (n=3, p=0.12). (**C**) Representative traces of single MEPPs and 1 s MEPP recordings in 4.5 and 10 mM K^+. MEPP amplitude and kinetics MEPPs were not affected by the S218L mutation. (**D**) Quantal content at 0.3 Hz stimulation frequency was similar in all genotypes (n=6, p=0.82). ω-Agatoxin-IVA (200 nM) reduced the quantal content by >90% in all three genotypes to almost identical levels (n=3). (**E**) Nerve stimulation-evoked ACh release at homozygous S218L KI NMJs is insensitive to the selective Ca_V channel blockers ω-conotoxin-GVIA (2.5 μM, $Ca_V2.2$, n=2), and SNX-482 (1 μM, $Ca_V2.3$, n=3), but reduced significantly by 200 nM of the $Ca_V2.1$ channel blocking toxin ω-agatoxin-IVA (n=3, $p<0.01$). † $p<0.01$, ‡ $p<0.001$.

Results

S218L KI mice

A phenotypical description of the generated S218L KI mice will be provided elsewhere. In short, mice were viable, but displayed symptoms of ataxia and tremor and had a reduced survival rate due to sudden death (~50% survival at 5 months of age). No overt epilepsy symptoms were present.

Increased spontaneous transmitter release at S218L neuromuscular synapses

A first series of experiments was performed with mice of ~2 months of age. Spontaneous uniquantal ACh release, measured as MEPP frequency was increased ~12-fold at homozygous S218L KI NMJs (1.24 ± 0.06 s^{-1} at wild-type and 15.50 ± 1.18 s^{-1} at KI NMJs, n=6, $p<0.001$; Figure 1A). Heterozygous KI NMJs showed an intermediate MEPP frequency of 10.56 ± 1.17 s^{-1} (n=6, $p<0.01$). The MEPP amplitude was ~1 mV under all conditions and did not differ between genotypes (n=6, p=0.17; Figure 1C), neither did MEPP rise times, decay times and halfwidth values (data not shown).

Occasionally, spontaneous twitches of individual muscle fibers were observed in homozygous S218L KI diaphragm preparations. They could be blocked by 1 μM d-tubocurarine. This suggests that the twitches resulted from occasionally superimposed MEPPs, due to their high frequency, reaching the firing threshold of the muscle fiber.

In order to asses the contribution of $Ca_V2.1$ channels to uniquantal release, we applied 200 nM ω-agatoxin-IVA to the preparation. Whereas MEPP frequency was reduced by ~60% at wild-type NMJs (0.48 ± 0.05 s^{-1}, n=3, $p<0.001$; Figure 1A), spontaneous release decreased by ~90% at heterozygous and homozygous S218L KI NMJs (to 1.08 ± 0.24 and 1.62 ± 0.08 s^{-1}, respectively; n=3, $p<0.05$; Figure 1A), indicating that the increased MEPP frequency in KI mice is most likely exclusively mediated by S218L-mutated $Ca_V2.1$ channels.

MEPP frequency increased ~10-fold upon slight depolarisation of the nerve terminals by raising K^+ to 10 mM (11.7 ± 1.4, 78.1 ± 13.2 and 150.3 ± 21.3 s^{-1} at wild-type, heterozygous and homozygous S218L NMJs, respectively; n=6, $p<0.01$; Figures 1B, C). The difference of MEPP frequency between genotypes remained similar (n=6, p=0.33), however, was abolished upon application of ω-agatoxin-IVA (n=3, p=0.12).

Quantal content is unaltered at S218L KI NMJs

When stimulating the phrenic nerve supramaximally at 0.3 Hz, the EPP amplitude was ~28 mV for all genotypes (n=6, p=0.28; data not shown). The quantal content, calculated from the corrected and normalized EPP and MEPP amplitudes, was ~40 in all groups and did not differ between genotypes (38.0 ± 2.5, 40.5 ± 2.6 and 39.8 ± 3.7 at wild-type, heterozygous and homozygous S218L NMJs, respectively; n=6, p=0.82; Figure 1D).

No compensatory contribution of non-$Ca_V2.1$ channels

We considered the possibility that as a result of the $Ca_V2.1$ mutation, other types of Ca_V channels may be expressed at the NMJ and contribute to evoked ACh release, as we described previously for the *tottering* P601L mutation (Kaja et al., 2006) and has been shown at $Ca_V2.1$ KO NMJs (Urbano et al., 2003). However, ω-agatoxin-IVA reduced quantal content equally in all genotypes by ~90% to 1.9 ± 0.1, 3.7 ± 0.5 and 4.6 ± 0.2 at wild-type, heterozygous and homozygous S218L KI NMJs, respectively (n=3, $p<0.05$; Figures 1D, E). The selective $Ca_V2.2$ (N-type) blocking toxin ω-conotoxin-GVIA (2.5 μM) did not have any effect on ACh release parameters at homozygous S218L KI synapses. Quantal contents were 46.2 ± 2.9 and 50.4 ± 0.5 before and after application of the toxin (n=2; Figure 1E). Similarly, quantal

contents were 40.7 ± 3.6 before and 39.9 ± 2.9 after incubation with 1 μM of the selective $Ca_V2.3$ (R-type) channel blocker SNX-482 (n=3, p=0.37; Figure 1E). MEPP frequency was not affected by either ω-conotoxin-GVIA or SNX-482 (data not shown).

Increased EPP rundown and reduced paired-pulse facilitation at S218L KI NMJs

Some changes of mutant $Ca_V2.1$ channel function may only be revealed at high-frequency use. We, therefore, measured ACh release following a high-frequency stimulus train (35 stimuli at 40 Hz). EPP amplitudes of wild-type were higher than those of both heterozygous and homozygous S218L KI mice at the end of a stimulus train (Figure 2A), resulting from an increased rundown of EPP amplitudes at S218L KI synapses compared with wild-type. The mean residual EPP amplitude at stimuli 21-35, expressed as percentage of the first EPP in the train, was 79.1 ± 1.9% (n=6, p=0.08) at heterozygous S218L KI NMJs and only 77.5 ± 0.9% (n=6, p<0.01) at homozygous KI synapses, when compared with wild-type NMJs, where rundown level was 83.4 ± 0.8 % (n=6; Figures 2B, C).

We looked at the first two EPPs of the stimulus train to assess 25 ms paired-pulse facilitation, a process of short-term synaptic plasticity. At the wild-type NMJ, amplitude of the second EPP was 103.7 ± 0.2% of the first EPP. Facilitation was somewhat lower in both heterozygous and homozygous S218L KI mice (101.1 ± 0.4 and 99.6 ± 0.3%, respectively; n=6, p<0.001, Figure 2D).

No (sub-)clinical muscle weakness in S218L mice

Block of transmission at the NMJ will result in muscle weakness. Although our electrophysiological measurements at the NMJ of diaphragms were not indicative of transmission block, the NMJ condition in extremity muscles might be different. However, when we assessed grip strength of the fore paws *in vivo*, no differences between genotypes were found. Wild-type, heterozygous and homozygous S218L KI mice pulled 92.5 ± 1.4, 93.2 ± 2.5 and 93.2 ± 1.9 g, respectively (n=5, p=0.96; data not shown).

We assessed a possible subclinical muscle weakness by testing the d-tubocurarine sensitivity of the 40 Hz nerve stimulation evoked tetanic force in *ex vivo* contraction experiments with diaphragm muscles. However, no differences were observed between S218L and wild-type preparations (Figure 2F). The absolute twitch and tetanic contraction forces in Ringer's medium without d-tubocurarine were equal (Figure 2G).

Higher quantal content at S218L KI NMJs at low extracellular Ca^{2+}

At physiological extracellular Ca^{2+} concentration, Ca^{2+} sensors of the neurotransmitter release machinery may approach saturation during action potential-induced Ca^{2+} influx (Schneggenburger and Neher, 2000). Therefore, transmitter release measured at lower extracellular Ca^{2+} concentration may better reflect the behaviour of (mutant) $Ca_V2.1$ channels. In our studies on the FHM1 R192Q *Cacna1a* KI NMJs, we identified a concentration of 0.2 mM Ca^{2+} as critical to unmask differences between mutant and wild-type $Ca_V2.1$ channel function (Van Den Maagdenberg et al., 2004; Kaja et al., 2005). We, therefore, measured ACh release at S218L KI NMJs also in low, 0.2 mM, extracellular Ca^{2+}.

MEPP frequencies were 0.35 ± 0.04, 0.85 ± 0.16 and 1.36 ± 0.18 s^{-1}, at wild-type, heterozygous and homozygous S218L NMJs, respectively (n=3, p<0.01; Figure 3A). MEPP amplitudes remained unchanged (data not shown). Furthermore, we found a gene-dosage dependent effect on 0.3 Hz evoked EPP amplitude and quantal content. EPP amplitudes were increased ~2-fold in heterozygous, ~3-fold at homozygous S218L KI NMJs, compared to wild-type (Figures 3B, D). Quantal contents were 7.2 ± 1.5, 13.9 ± 0.7 and 18.3 ± 1.7 at wild-type, heterozygous and homozygous S218L NMJs, respectively (n=3, p<0.01; Figure 3C).

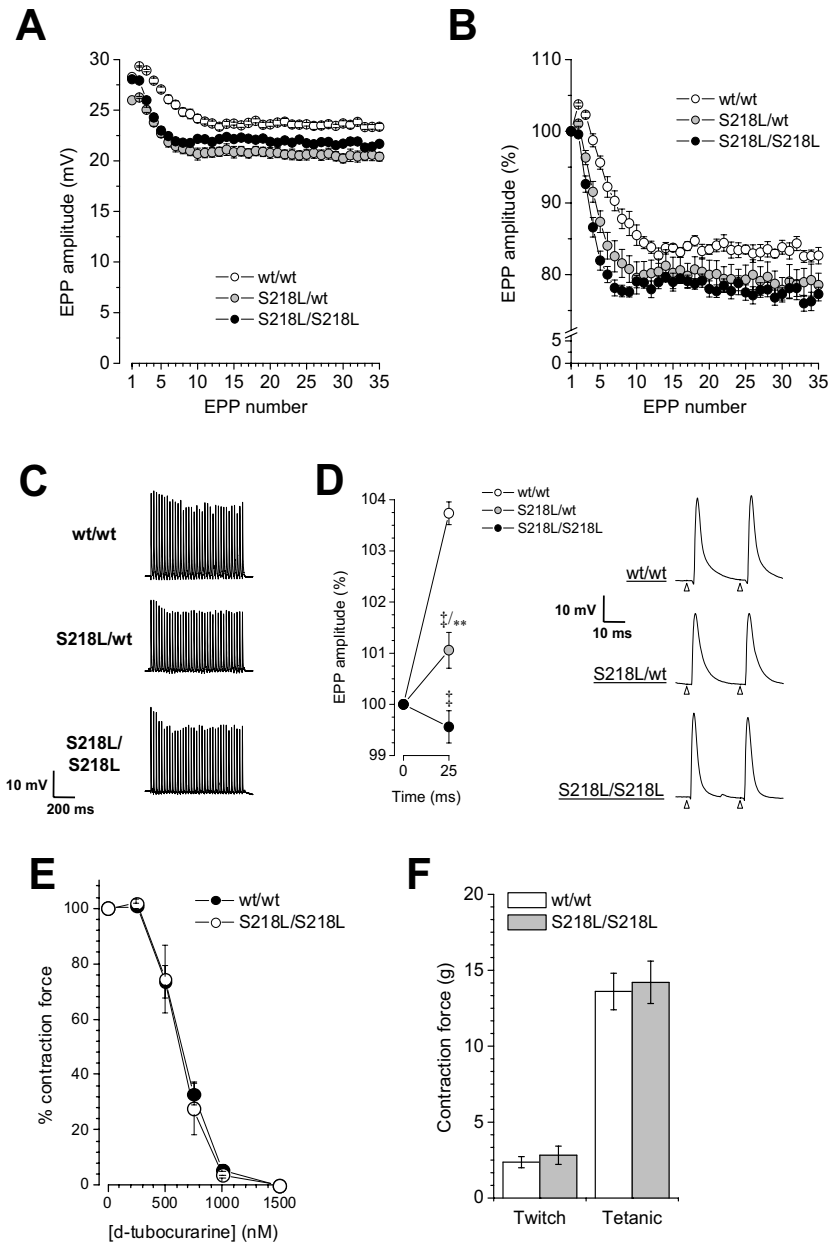

Figure 2. S218L KI synapses show increased EPP amplitude rundown at high-frequency (40 Hz) stimulation, reduced paired-pulse facilitation and normal sensitivity of nerve stimulation-evoked contraction to d-tubocurarine (d-TC).
(**A, B**) EPP amplitudes run down to lower levels at heterozygous and homozygous S218L KI NMJs. The plateau levels, determined as the mean EPP amplitude of EPPs $_{21\text{-}35}$ expressed as a percentage of the first EPP in a train, were 83.4 ± 0.8, 79.1 ± 1.9, and 77.5 ± 0.9 at wild-type, heterozygous and homozygous S218L KI NMJs (n=6, $p<0.05$). (**C**) Representative examples of 40 Hz EPP rundown profiles. (**D**) Paired-pulse facilitation (25 ms interval) is reduced at homozygous S218L KI synapses (n=6, $p<0.001$). Heterozygous synapses show an intermediate facilitation (n=6, $p<0.001$). Representative traces of 25 ms paired-pulse evoked EPPs are shown. (triangle indicates the moment of nerve stimulation.) (**E**) d-TC sensitivity of nerve stimulation-evoked tetanic contraction in *ex vivo* experiments was similar in diaphragms of wild-type and S218L/S218L mice (n=5,). (**F**) The absolute twitch force (n=3-4) and tetanic force (n=5) generated by S218L/S218L diaphragms is unchanged. † $p<0.01$, ‡ $p<0.001$, different from wild-type; ** $p<0.01$, different from S218L/S218L.

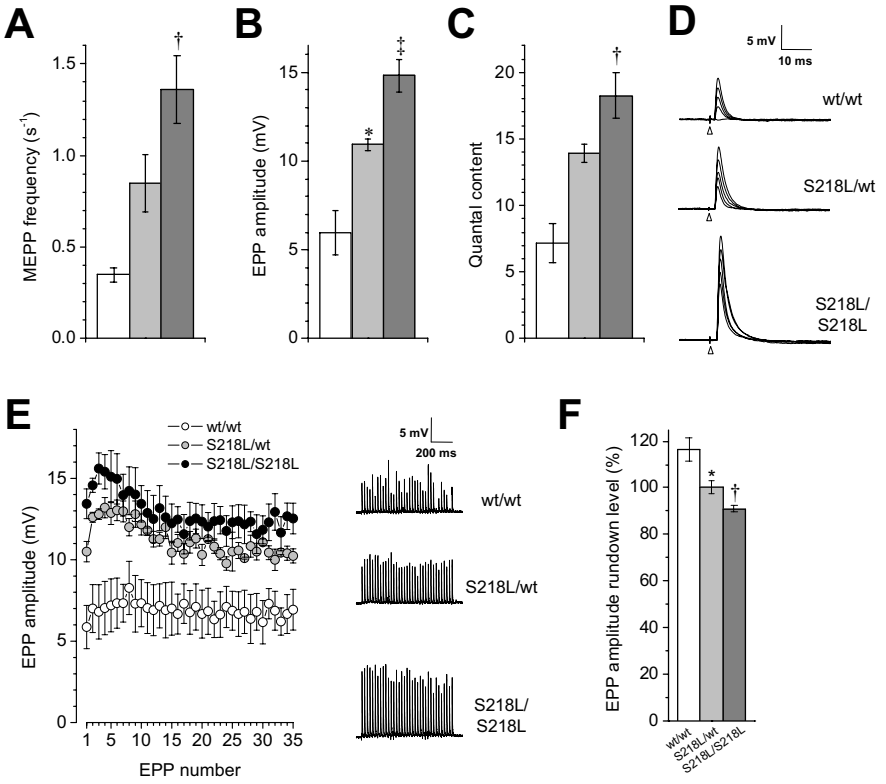

Figure 3. ACh release at low (0.2 mM) extracellular Ca^{2+} is increased at S218L KI NMJs.
(**A**) MEPP frequency is increased ~3-fold at homozygous (S218L/S218L, n=3) and ~2-fold at heterozygous (S218L/wt, n=3) S218L KI NMJs compared with wild-type (wt/wt), when measured in 0.2 mM Ca^{2+} in the Ringer's medium. (**B**) Similarly, EPP amplitudes are higher in S218L-mutated synapses. (**C**) Compared to wild-type, quantal content at 0.2 mM Ca^{2+} is ~150% higher in homozygous S218L KI mice (n=3, $p<0.01$) . (**D**) Representative examples of 0.3 Hz EPPs at 0.2 mM Ca^{2+}. Under these conditions, failures of transmission are observed frequently at wild-type, however, not at S218L KI NMJs. Triangles indicates the moment of nerve stimulation. (**E**) EPP rundown profiles at 40 Hz stimulation in the presence of 0.2 mM Ca^{2+}. Representative example traces (1 s, 40 Hz) are shown. (**F**) The plateau level of EPP rundown is significantly lower in heterozygous (n=3, $p<0.05$) and homozygous (n=3, $p<0.01$) S218L KI mice, compared with wild-type. $^{*}p<0.05$, $^{\dagger}p<0.01$, $^{\ddagger}p<0.001$.

EPP rundown at 40 Hz stimulation differed between genotypes in a gene-dosage dependent fashion (Figures 3 E, F). The mean amplitude of the last fifteen EPPs in the train, expressed as percentage of the first EPP, was 116.4 ± 4.9, 100.2 ± 3.0 and 90.9 ± 1.4% at wild-type, heterozygous and homozygous NMJs, respectively (n=3, $p<0.05$; Figure 3G).

Synaptic defects at S218L KI NMJs progress with age

Long-term synaptic changes and damage may occur as a result of prolonged presynaptic Ca^{2+} influx. Measuring ACh release at NMJs of mice of 4.5 and 12 months of age, we compared the magnitude of changes compared with age-matched wild-type littermates (Figure 4A).

MEPP frequency at homozygous S218L KI NMJs of mice of 4.5 month of age was 3-fold higher than at 2 months of age, corresponding to a >20-fold increase compared with 4.5 months old wild-types (Figures 4A, B). MEPP frequency was 47.8 ± 7.7 and 2.1 ± 0.2 s^{-1} at S218L KI and wild-type NMJs, respectively (n=4, $p<0.001$; Figure 4B). At NMJs of 12 months of age, the difference between S218L KI and wild-type mice was similar to the one observed at 2 months of age (n=5, p=0.32; Figures 4A, B).

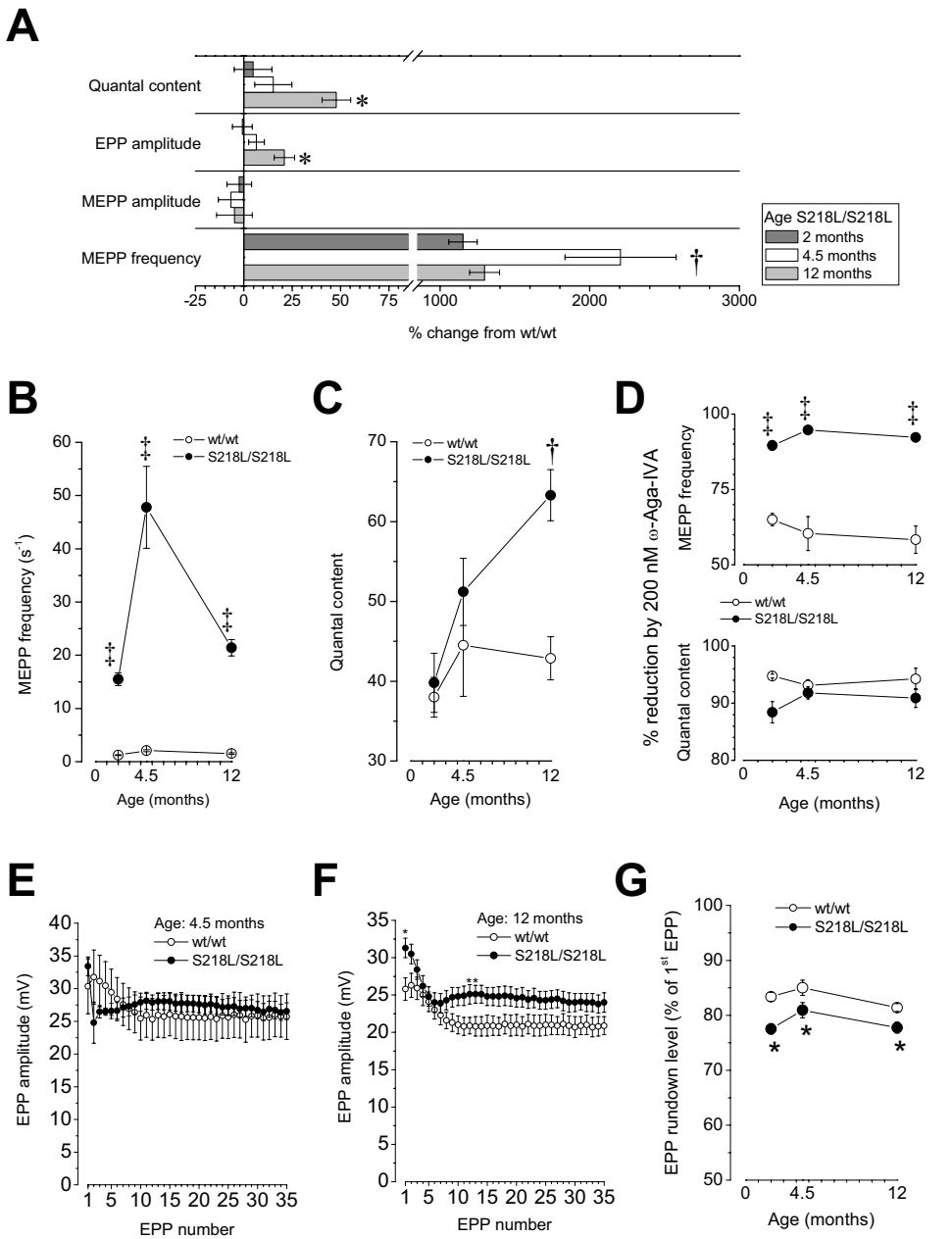

Figure 4. Age-related changes in ACh release at S218L KI NMJs.
(**A**) Magnitude of electrophysiological changes at S218L KI NMJs, compared with wild-type. (**B**) S218L KI MEPP frequency was increased ~12-fold at 2 months (n=6, p<0.001), ~22-fold at 4.5 months (n=4, p<0.001) and ~13-fold at 12 months of age (n=5, p<0.001). (**C**) Quantal content was similar to wild-type, in 2 months-old mice, however, and became increased in older S218L KI mice. This difference became statistically significant at 12 months of age, where quantal content was 48% higher at S218L KI NMJs (n=5, p<0.01). (**D**) Sensitivity of both MEPP frequency (top panel) and quantal content (bottom panel) to 200 nM of the $Ca_V2.1$-selective channel blocking toxin ω-agatoxin-IVA remained similar across all ages measured, indicating that S218L terminals do not develop compensatory contribution of other non-$Ca_V2.1$ channels. (**E**) Rundown of EPP amplitude at 40 Hz stimulation at 4.5 months of age. (**F**) Rundown of EPP amplitude at 40 Hz stimulation at 12 months of age. (**G**) EPP rundown level defined as mean amplitude of EPP_{21-35}, expressed as percentage of the first EPP of the train, was lower at S218L KI NMJs at all ages measured, when compared with wild-type. $^{*}p<0.05$, $^{\dagger}p<0.01$, $^{\ddagger}p<0.001$.

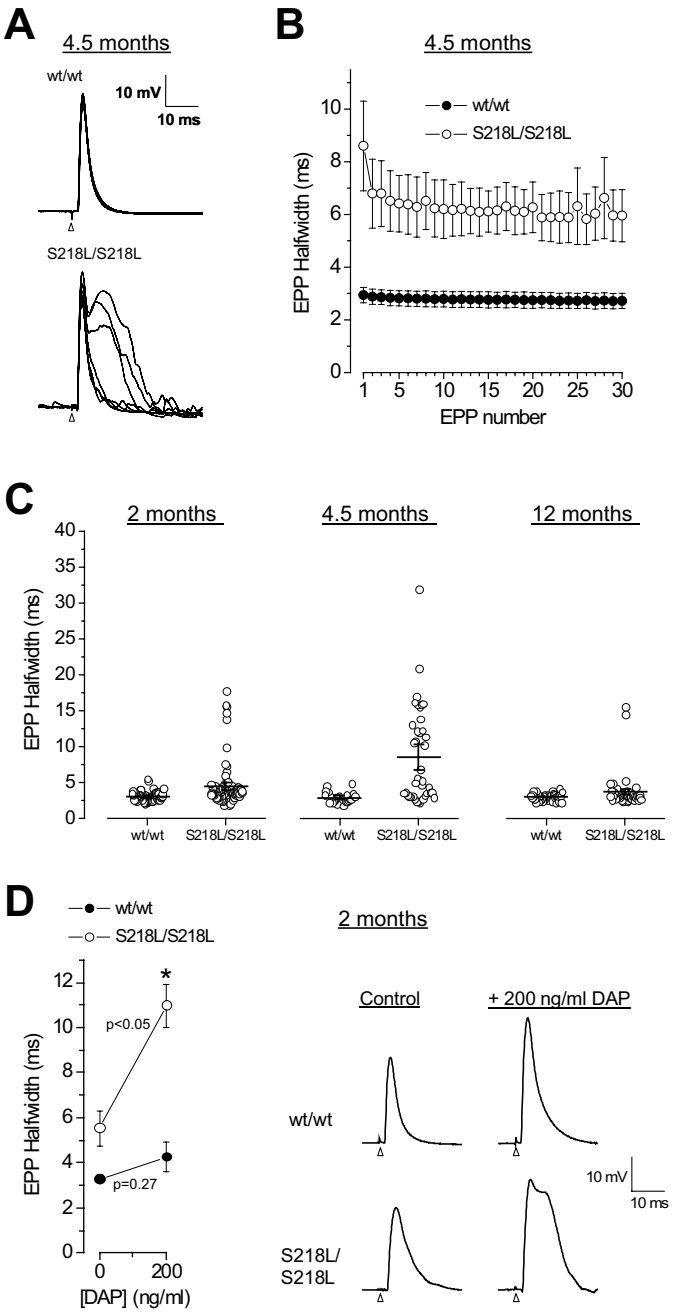

Figure 5. Increased EPP half-widths at S218L KI NMJs.
(**A**) Representative EPP recordings obtained at wild-type and S218L KI NMJs from 4.5 months-old mice (triangle indicates the moment of nerve stimulation). (**B**) Development of EPP half-width during a 0.3 Hz stimulation at NMJs from 4.5 months-old mice. EPP half-width is increased ~2-fold compared with wild-type (n=4, $p<0.05$). (**C**) Half-widths of the first EPP measured at 0.3 Hz stimulation, plotted as scatter graphs of individual NMJ values, at 2, 4.5 and 12 months of age. (**D**) EPP half-width (mean of the first EPP measured at 0.3 Hz stimulation) of 2 months-old wild-type mice was insensitive to application of 200 ng/ml 3,4-diaminopyridine (DAP) (n=3, $p=0.27$). At S218L KI synapses, however, EPP half-width doubled compared with control (n=5, $p<0.05$). Representative single EPP recordings are shown for both genotypes before application and in the presence of 200 ng/ml DAP (triangle indicates the moment of nerve stimulation). $^{*}p<0.05$, $^{\dagger}p<0.01$

Quantal content at S218L NMJs of 4.5 months old mice was similar to wild-type, whereas at 12 months of age it was ~50% higher than at age-matched wild-types (n=4, $p<0.01$).

In order to test the possibility of long-term compensatory contribution of non-$Ca_V2.1$ channels, we applied 200 nM ω-agatoxin-IVA to the preparation. However, ω-agatoxin-IVA-sensitivity did not change with increasing age (Figure 4D).

At 40 Hz stimulation, the difference in EPP amplitude rundown level between S218L and wild-type NMJs remained similar at the different ages (Figures 4E-G).

Increased EPP half-width in S218L KI mice

When measuring neurotransmitter release at homozygous S218L synapses, we encountered very broad EPPs, occasionally (at NMJs of 2 months-old mice) and frequently (at NMJs of 4.5 months-old mice). Representative traces obtained at 4.5 months of age are shown in Figure 5A. Also, there appeared to be large variation in EPP halfwidth during 0.3 Hz stimulation, in general becoming less pronounced during the stimulation period (Figure 5B). This phenomenon might possibly result from mechanisms causing channel inactivation and recovery from inactivation (Lee et al., 1999).

Interestingly, EPP halfwidth showed a similar progression with age as fMEPP: mean EPP halfwidths (first EPP at 0.3 Hz stimulation) at wild-type and S218L KI synapses, respectively, were 3.14 ± 0.15 and 4.54 ± 0.58 ms (at 2 months of age; n=9-11, $P<0.05$), 2.94 ± 0.29 and 8.60 ± 1.70 ms (at 4.5 months of age; n=4, $P<0.01$), and 3.09 ± 0.07 and 3.76 ± 0.32 ms (at 12 months of age; n=5, P=0.08; Figure 5C).

The broadening of EPPs observed in S218L KI synapses appeared similar to EPP broadening in the presence of the selective blocker of pre-synaptic K^+ channels, 3,4-diaminopyridine (DAP), which causes prolonged opening of $Ca_V2.1$ at the NMJ (Katz and Miledi, 1979). We speculated that S218L KI EPP halfwidth should be more sensitive to application of DAP, were the EPP broadening observed under physiological conditions a result of increased Ca^{2+} influx through S218L-mutated $Ca_V2.1$ channels. Indeed, application of 200 ng/ml DAP in the Ringer's medium resulted in an ~100% increase in EPP halfwidth in 2 months old S218L KI mice, whereas halfwidths at wild-type synapses were not affected. Halfwidths at wild-type NMJs were 3.30 ± 0.16 and 4.26 ± 0.67 ms before and after application of DAP, respectively (n=3, P=0.27), and 5.54 ± 0.78 and 10.97 ± 0.96 ms at S218L KI NMJs, respectively; n=5, $P<0.05$; Figure 5D).

Similar neuromuscular synaptic phenotype in other types of muscles

The diaphragm consists of a mixed population of slow- and fast-twitch muscle fibers, with different NMJ characteristics (Bewick, 2003), and thus may be influenced differentially by the S218L mutation. We, therefore, also assessed ACh release at NMJs of soleus (exclusively slow-twitch muscle fibers) and FDB (fast-twitch) muscle preparations of wild-type and S218L KI mice at 4.5 months of age.

MEPP frequency was 2.25 ± 0.01 and 47.77 ± 21.23 s^{-1} at wild-type and S218L KI soleus NMJs, respectively (n=2) and similar to those found in diaphragm (Figure 4B). Similarly to diaphragm, when subjected to slightly depolarizing medium (10 mM K^+), MEPP frequency at soleus wild-type and S218L KI NMJs increased to 25.2 ± 1.8 and 187.2 ± 38.5 s^{-1}, respectively (n=2). Quantal contents were 56.9 ± 0.6 and 68.1 ± 9.4 at soleus wild-type and S218L KI NMJs, respectively (n=2; data not shown). At high rate (40 Hz) stimulation, EPP amplitude rundown was slightly more pronounced at S218L KI synapses compared with wild-type (to 70.0 ± 4.9 and 78.8 ± 2.2%, of the first EPP respectively; n=2).

At S218L FDB NMJs MEPP frequency was measured and found increased ~20-fold compared to wild-type (25.75 ± 4.22 and 1.27 ± 0.21 s^{-1}, respectively, n=2).

Unchanged S218L NMJ size

The functional changes at S218L NMJs could possibly also result from changes in morphology and, *vice versa*, could themselves lead to morphological changes. Because NMJ size is an important determinant of the level of ACh release (Kuno et al., 1971; Smith, 1984), we quantified this parameter with fluorescence microscopy in diaphragms of two months-old

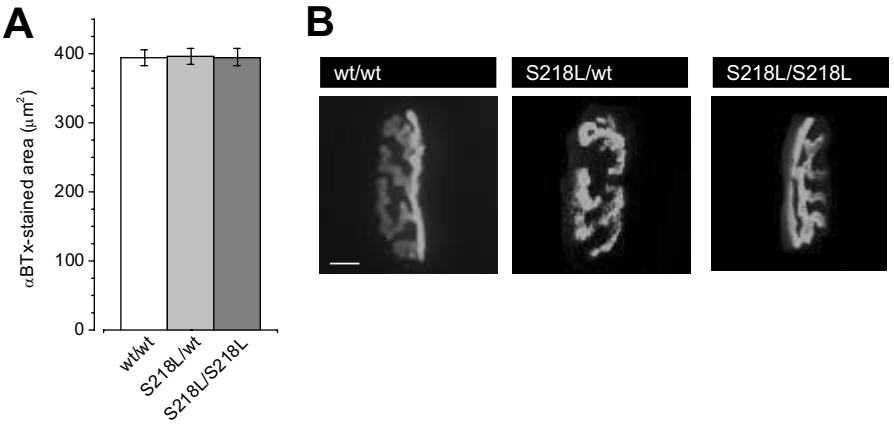

Figure 6. No change in S218L KI NMJ size.
(**A**) Area of fluorescently-labeled ACh receptors is similar at 2 months-old wild-type, heterozygous and homozygous S218L KI NMJs (n=3-5). Perimeter, length and width of NMJs were also unchanged (data not shown). (**B**) Representative images of fluorescent α-bungarotoxin-stained NMJs (scale bar = 15 μm).

mice. However, no differences were identified: areas of αBTx-stained NMJs were 394.0 ± 12.0, 395.4 ± 11.5 and 394.9 ± 11.8 μm² at wild-type, heterozygous and homozygous S218L KI diaphragm NMJs, respectively (n=3-5, p=0.99; Figures 6A, B).

Discussion

We investigated neurotransmitter release at NMJs of a newly generated KI mouse strain carrying the human S218L mutation in CACNA1A-encoded $Ca_V2.1$ channels, identified in families suffering from FHM1 with susceptibility for coma and brain edema after mild head trauma. Our studies indicate that S218L-mutated $Ca_V2.1$ channels mediate increased and prolonged presynaptic Ca^{2+} influx, leading to increased neurotransmitter release. The observed changes were gene dosage-dependent and progressed with age, but did not lead to muscle weakness or morphological synaptic abnormalities. As elaborated below, similarly increased transmitter release at central synapses may contribute to the neurological phenotype of S218L mutated mice and humans.

Increased spontaneous ACh release from S218L KI motor-nerve terminals

S218L KI NMJs showed an increase in spontaneous ACh release under normal and mildly depolarizing (10 mM K^+) conditions. This may result from a negative shift in activation voltage of putative *Cacna1a*-encoded low voltage-activated $Ca_V2.1$ channels, as proposed by us previously (Plomp et al., 2000; Kaja et al., 2005). The hypothesis of a negatively shifted activation voltage is supported by findings in both cultured primary cerebellar granule cell

neurones from S218L KI mice (D. Pietrobon, personal communication) and heterologous expression systems (Tottene et al., 2005), where a negative change in the half-maximal activation voltage of ~10 mV was found for S218L-mutated channels. Compensatory contribution of non-$Ca_V2.1$ channels to spontaneous release is unlikely, because the relative increase compared to wild-type was blocked entirely by the $Ca_V2.1$ selective channel blocker ω-agatoxin-IVA. Furthermore, $Ca_V2.2$- and $Ca_V2.3$-specific blocking toxins had no effect on MEPP frequency.

We have previously reported increased spontaneous ACh release also for a number of other *Cacna1a* mutants with single amino acid changes, namely the spontaneous mutants *tottering* (Plomp et al., 2000; Kaja et al., 2006) and *rolling Nagoya* (Plomp et al., 2003; chapter 6), and for the transgenic FHM1 R192Q KI strain (Van Den Maagdenberg et al., 2004; Kaja et al., 2005). All these mutations are localized at or near voltage-sensing segments of $Ca_V2.1$. However, increased MEPP frequency was also observed in NMJs of biopsied muscle in an EA2 patient with a CACNA1A *truncation* mutation (Maselli et al., 2003a), indicating that there might be more than one type of functional change leading to increased Ca^{2+} influx under resting condition.

Increased evoked ACh release at S218L KI synapses

We observed clear changes in nerve stimulation-evoked ACh release at S218L KI NMJs, compared with wild-type. Evoked ACh release (0.3 Hz) under physiological conditions was not different between genotypes at NMJs of young mice, however, reached ~150% of wild-type levels at 12 months of age. Furthermore, S218L KI NMJs had a 3-fold higher quantal content than wild-type in low (0.2 mM) Ca^{2+}.

As with spontaneous release, these increases in evoked release are compatible with a negative shift in activation potential of $Ca_V2.1$ channels induced by the S218L mutation, as demonstrated in the transfection studies (Tottene et al., 2005). Furthermore, reduced inactivation of S218L-mutated channels, as also observed in the expression studies (Tottene et al., 2005) may contribute. Other mechanisms might include altered Ca^{2+}/calmodulin-dependent channel inactivation (Lee et al., 1999), or different G-protein activation, as shown for the FHM1 R192Q mutation (Melliti et al., 2003).

Increased EPP halfwidth indicates prolonged opening of S218L $Ca_V2.1$ channels

Broadened EPPs were observed frequently in S218L KI mice. EPP broadening is a feature of inhibition or absence of acetylcholinesterase at the NMJ (Burd and Ferry, 1987; Hutchinson et al., 1993). If this were the case, due to some indirect effect of the mutation, the halfwidth of uniquantal responses (MEPPs) should, however, also have been found increased. Since this was not the case, the most likely explanation for EPP broadening is prolonged open duration of the S218L-mutated $Ca_V2.1$ channels upon activation by a nerve action potential. The EPP halfwidths at S218L KI NMJs of 2 months old mice being more potentiated by 200 ng/ml DAP than wild-types supports this hypothesis.

There was large variation in EPP halfwidths between NMJs within the same S218L KI diaphragm, and a considerable part of the NMJs still had wild-type values. The change in EPP halfwidth may possibly be related to muscle fiber type. As mentioned above, the diaphragm consists of a mixed population of slow- and fast-twitch muscle fibers, with differential NMJ characteristics. In this respect it is of interest to note that the (more limited) analysis of EPPs at NMJs of soleus muscles, which consist exclusively of slow-twitch fibers, did not reveal an increase in halfwidth (data not shown).

S218L-Ca_V2.1 channel dysfunction at high-frequency use

We observed a slightly more pronounced rundown of EPP amplitudes upon high-frequency use (40 Hz stimulation) at S218L than at wild-type NMJs. Physiological EPP rundown is most likely due to a combination of Ca_V2.1 channel inactivation and replenishment rate of synaptic ACh vesicles. Most likely, the extra rundown at S218L NMJs is caused by increased channel inactivation and reduced rate of recovery. Such S218L-Ca_V2.1 characteristics were indeed shown in transfected cells (Tottene et al., 2005). The somewhat reduced 25 ms paired-pulse facilitation at S218L KI NMJs may hint towards increased Ca^{2+}/calmodulin dependent inactivation (Lee et al., 1999) at S218L KI NMJs induced by increased Ca^{2+} influx through mutated Ca_V2.1 channels during the first pulse.

The slightly increased 40 Hz EPP rundown will reduce the safety factor of neuromuscular transmission, although the extent of which is probably not large enough to cause transmission block. However, one would expect increased d-tubocurarine sensitivity of the 40 Hz nerve stimulation evoked muscle contraction of S218L diaphragm *ex vivo*, but this was not found. Most likely, the increased EPP halfwidths and slightly increased initial quantal content compensated for the mildly increased amplitude rundown.

Transmitter release abnormalities are gene-dosage dependent and progressive

We observed a gene-dosage effect on several ACh release parameters, i.e. values of MEPP frequency, quantal content in low Ca^{2+}, EPP halfwidth and 40Hz EPP amplitude rundown of heterozygous NMJs were intermediate to wild-type and homozygous S218L values. This indicates that S218L-mutated Ca_V2.1 channels co-exist with wild-type channels in the heterozygous condition and exclude a complete dominant-negative effect of the mutated channels. A gene-dosage dependency of a similar synaptic phenotype at brain synapses may underlie the autosomal dominant inheritance pattern of the S218L-FHM1 symptoms (Kors et al., 2001).

Some S218L NMJ parameters showed age-dependent fluctuation in their extent of difference with wild-type. MEPP frequency and EPP halfwidth increases were highest in 4.5 months-old mice, but again lower in 12 months-old animals. Given the reduced survival rate, the 12 months age group consists of "survivors", possibly with a synaptic phenotype biased towards the wild-type conditions. The 0.3 Hz quantal content, however, became increased at NMJs of 12 months-old KI mice. One possible explanation may be a differential response of S218L KI NMJs to maturation. The level of neurotransmitter release at the NMJ increases with age in both humans (Wokke et al., 1990) and rodents (Smith, 1984), and is correlated with nerve terminal branching and overall NMJ size (Kuno et al., 1971; Smith, 1984). However, fluorescence microscopical quantifications did not show changed overall NMJ size at 2 months of age. Electron microscopical studies of aged S218L KI NMJs will be needed to reveal possible ultrastructural changes. A similar progression of evoked neurotransmitter release at some CNS synapses may be beneficial for survival of S218L KI mice. Long-term increased pre-and postsynaptic Ca^{2+} influx may have deleterious effects on synapse function (Mattson et al., 1998). Apoptosis pathways may become activated when cytosolic Ca^{2+} buffer systems saturate, resulting in synapse degeneration. At the NMJ, prolonged stimulation of post-synaptic ACh receptors might cause muscle fiber damage similar to that seen in the slow-channel syndrome (Vohra et al., 2004), following from particular ACh receptor mutations. Again, electron microscopical analysis of aged NMJs might be informative.

No functional compensation for S218L-mutated Ca_V2.1 channels

It has been shown that non-Ca_V2.1 channels can compensate for mutated or absent Ca_V2.1 channels, either in the CNS (Inchauspe et al., 2004; Cao et al., 2004) or at the NMJ (Urbano

et al., 2003; Kaja et al., 2006; cf. chapters 5 and 7). For instance, P601L-mutated *tottering* mice exhibited reduced $Ca_V2.1$-mediated evoked ACh release at the NMJ that was fully compensated for by $Ca_V2.3$ channels (Kaja et al., 2006). However, no compensatory contribution of non-$Ca_V2.1$ channels was found at R192Q KI NMJs (Van Den Maagdenberg et al., 2004; Kaja et al., 2005). Here, at S218L KI NMJs, experiments with selective $Ca_V2.1$ channel blocking toxins did not indicate compensatory contribution of non-$Ca_V2.1$ channels to ACh release. This finding, however, does not exclude the possibility that some central synapses may exhibit functional compensation.

Usefulness of S218L KI mice as animal model for FHM1

The findings at CACNA1A S218L KI NMJs show similarity to those at FHM1 R192Q KI mice: increased spontaneous ACh release, increased evoked release at low extracellular Ca^{2+}, subtle reduction of high frequency evoked ACh release and the absence of compensatory contribution of non-$Ca_V2.1$ channels (Van Den Maagdenberg et al., 2004; Kaja et al., 2005). However, the S218L mutation has much more severe consequences in mice, including a neurological phenotype of ataxia, reduced survival and synaptic changes that are the likely result of prolonged opening of mutated $Ca_V2.1$ channels, in accordance with a much more severe phenotype in patients with the S218L mutation (Ophoff et al., 1996; Kors et al., 2001).

The neuromuscular synaptic phenotype provides for some speculative extrapolation to the situation in the S218L $Ca_V2.1$-mutated CNS. Of interest, $Ca_V2.1$ channels are involved in many areas associated with migraine and nociception, including brainstem, cortex and trigeminal system (for reviews, see Goadsby, 2005; Pietrobon, 2005a). We have hypothesized previously that increased spontaneous neurotransmitter release might affect dendritic integration of inhibitory and excitatory evoked responses, which are of low amplitude (Stevens, 1993). Increased transmitter release in the cerebellum may contribute to the ataxic phenotype of S218L KI mice, because cerebellar synapses are mainly dependent on $Ca_V2.1$ channels (Mintz et al., 1992a; Mintz et al., 1995) and evoked release is generally low (Hessler et al., 1993). This situation is thus comparable with ACh release at NMJs at low Ca^{2+}, which is several-fold increased in S218L KI mice, compared with wild-type. Similarly, increases in $Ca_V2.1$ channel-mediated neurotransmitter release of glutamatergic cortical synapses may trigger or maintain cortical spreading depression, the mechanism underlying migraine aura, and activation of the trigeminal system, which is supposedly responsible for migraine headache, as suggested, as hypothesized by us and others previously (Van Den Maagdenberg et al., 2004; Kaja et al., 2005; Pietrobon, 2005a).

Besides these possible insights into migraine pathophysiology, S218L KI mice might be used in the study of new anti-ataxia/migraine drugs.